

Modeling nonthermal plasmas generated in glow discharges*

I. Revel, Ph. Belenguer, J. P. Boeuf and L. C. Pitchford†

*Centre de Physique des Plasmas et Applications de Toulouse (CPAT),
118 route de Narbonne, 31062 Toulouse, France*

Abstract: Over the past decade, tremendous progress has been made in the modeling of nonthermal plasmas, and models have now reached the point that they are being used to help guide the experimental optimization of plasma based devices. In this communication we provide an overview of models used to describe nonthermal plasma generated in glow discharges. We show results from two applications, plasma display panels and glow discharge mass spectrometry for materials analysis.

INTRODUCTION

The aim of this paper is to illustrate the impact of modeling on the development of plasma technology. We will focus on nonthermal plasmas. The modeling of these plasmas is rather intricate because it involves a description of the charged particle transport coupled with the electromagnetic field equations, with the kinetics of excited species (volume and surface reactions), photon transport and gas flow. Because of this complexity there is no ‘standard’ model of nonequilibrium plasma, and the model assumptions and equations depend on the particular device which is simulated. The ultimate goal of modeling is obviously to provide a quantitative prediction of the physical properties and performances of a particular device, but models can be very useful even if they can only predict the trends or help us understand the regime of operation of a particular device. In trying to develop accurate ‘quantitative models’, one must also keep in mind that the complexity of the model must be consistent with the uncertainties in some of the input data. Some of the fundamental data in a discharge model are not well known (e.g. secondary electron emission coefficient under ion impact on the surfaces, collision cross-sections or reaction rates between excited species, . . .) and whatever the details included in the model, the global accuracy of its predictions will be limited by these uncertainties in the input data [1].

MODELS

The modeling of non-equilibrium plasma is centered on the description of electron transport since the energy is deposited in these plasmas mainly by electrons through electron-neutral collisions. The transport of charged particles can be described using ‘particle models (PIC-MCC)’, ‘fluid models’ or ‘hybrid models’.

A PIC-MCC model (Particle-In-Cell + Monte Carlo-Collisions, [2]) would be the most accurate way of describing the electron and ion transport in the discharge cell in the self-consistent electric field. In a PIC-MCC the space and time dependent charged particle kinetic equations (Boltzmann equation) are solved by simulating the trajectories of a large sample of electrons and ions in phase space. The transport of a particle between collisions is obtained by time integration of the particle trajectory under the action of the electric field. The time and nature of the collisions are decided by using random numbers whose distributions are related to the collision cross-sections. The electric field is calculated at each time step

*Lecture presented at the 14th International Symposium on Plasma Chemistry, Prague, Czech Republic, 2–6 August 1999, pp. 1809–1918.

†Corresponding author: E-mail: leanne@cpa01.ups-tlse.fr

from the charged particle density distributions. This method provides the space and time variations of the charged particle velocity distribution functions but is very time consuming. This method although accurate is therefore not very practical for the simulation of real devices.

'Fluid models' are an alternative to the 'Particle models' described above. In fluid models only macroscopic properties of the charged particles are considered, i.e. density, average velocity and average energy. The corresponding equations are the continuity, momentum, and energy equations. These equations are obtained by taking moments of the Boltzmann equation in velocity space and describe respectively the charged particle growth, momentum exchange and energy exchange [3]. However this system of moment equations is not closed since some quantities appearing in these equations cannot be expressed as a function of charged particle density, velocity or mean energy. This is the case, for example, for the average frequencies that appear in these equations (e.g. ionization frequency, momentum exchange frequency, energy exchange frequency [3]). The frequencies are averaged over the electron (or ion) energy distribution function which is unknown since Boltzmann equation is not solved. The main approximation that must be made in a fluid description of electron and ion transport, is therefore related to the shape of the charged particle energy distribution function. A possible choice is to assume that the distribution is Maxwellian. This is a good approximation in a discharge close to thermal equilibrium but this approximation is generally not appropriate for the conditions of discharges, which are very far from thermal equilibrium. A better approximation is to assume that the distribution function at a given point and time has the same shape as under a uniform 'effective' electric field (swarm distribution). The value of this 'effective field' is chosen in such a way that the mean energy is the same as the mean energy at the considered point and time in the simulation. This method has the advantage of giving the accurate results during the breakdown phase in a particular device, i.e. when the electric field is not too much distorted by the space charge, whereas use of a Maxwellian distribution may lead to a rather wrong value of the breakdown voltage.

The fluid models becomes even simpler when one can use the Local Field Approximation (LFA) which assumes that the electron (or ion) distribution function at a given location and time is the same as the distribution corresponding to a uniform electric field for the value of the electric field which exists at this location and time in the discharge (see, e.g. [1]). In that case the frequencies and other transport parameters can be pre-tabulated as a function of the electric field (more precisely as a function of the reduced electric field E/N , field over gas density, of E/p , field over gas pressure) and no energy equation is needed. This implicitly assumes that the energy gain due to the field is locally (in space and time) balanced by energy losses due to collisions.

Under some discharge conditions, it may happen that none of the three possible approximations of the charged particle energy distribution function (EDF) described above (Maxwellian EDF, 'swarm' EDF, or LFA) are accurate enough. This is the case, for example, in the sheath and negative glow region of a DC discharge for large applied voltages, or in a hollow cathode discharge. When none of these approximations is adequate, a possible compromise is to use a hybrid model [3], i.e. a model where the low energy electrons are described with a fluid model, but where the energetic electrons responsible for ionization and excitation are described with a Monte Carlo simulation. In that case the model provides the high energy part of the electron distribution function and therefore the calculation of the ionization or excitation frequency is much more accurate, even for large variations of the electric field over distances on the order of the electron mean free path. In hybrid models one tries to combine the simplicity and computation efficiency of fluid models with the accuracy of kinetic models. The hybrid model is less demanding than a full particle model because one generally needs to describe accurately only the high energy part of the electron distribution (where electron impact ionization or excitation occurs). We will show some examples of results from hybrids and fluid models in the following.

Another issue that determines the complexity of the model, is the coupling between the charged particle transport and the plasma chemistry. It is clear that the plasma chemistry is completely dependent on electron transport since the source terms of the plasma chemistry equations are the electron impact excitation rates. On the other hand it is not always clear whether the presence of excited species strongly influences the electric part of the model (charged particle transport–electric field). This influence increases with increasing current density because the relative concentration of excited species (and

therefore the number of stepwise ionization events, superelastic collisions,...) increases with current density.

PLASMA DISPLAY PANELS

Plasma Display Panels (PDPs) are flat displays in which each picture element consists of microdischarges emitting VUV photons which are converted into visible (red, green, blue) by phosphors deposited on the discharge walls. The industrial production of PDPs for large area wall hanging televisions is now underway. However research is still needed to lower the power consumption and to improve the luminous efficiency and the contrast ratio of these displays. Numerical models of PDP discharge cells have been developed over the last few years and can help guide the optimization of these devices.

PDP cells operate in a high-pressure transient glow discharge regime (pressure on the order of 500 torr, gap length on the order of 100 μm), and fluid models are appropriate under these conditions. The approximations of the models are described, e.g. in [1].

Most of the PDP development is now done on AC systems where the electrodes are covered with dielectrics. The discharge occurring in these devices is a dielectric barrier glow discharge. The 'ON state' of a particular discharge cell is a succession of transient discharges at twice the frequency of the applied voltage (sustain voltage, frequency on the order of 100 kHz). The sustain voltage is applied constantly between the electrodes and is lower than the breakdown voltage so that the cells are in the 'OFF state' until a 'write pulse' is applied. To turn on a particular cell, a voltage pulse (above breakdown voltage) is applied between the electrodes of that cell. A discharge is initiated. The discharge is quickly quenched due to the presence of the dielectric layers above the electrodes. At the next half cycle, a new discharge is initiated because the voltage due to the charges ('memory charges') deposited on the dielectric layers during the previous discharge pulse now adds to the applied voltage. To turn off the cell one must cancel the memory charges that have been deposited by the write pulse.

Models have been used to study the gas breakdown and plasma formation and evolution in typical PDP conditions. Punset *et al.* [4] showed the influence of the geometry on the electrical and optical cross talk between adjacent PDP cells in 'matrix' geometries where the discharge occurs between electrodes on opposite planes. This same model was used in [5] to examine questions related to addressing cells in a coplanar geometry where the discharge occurs between electrodes on the same plane and a third electrode, on the opposite plane, is used to select a particular cell. Models have also been useful in characterizing the electron energy balance during the discharge pulse [6]. The calculations show that for a mixture of 10% xenon in neon, about 15% of the total energy is spent in excitation of xenon by direct electron impact. A large part of the total energy (as large as 60%) is spent into accelerating ions in the sheath region. This energy is lost in gas and surface heating. The rest of the energy is spent into ionization of xenon and neon, and into neon excitation. Much of the energy deposited in excitation of xenon is then used for UV photon production. The xenon metastable and resonant states are populated by direct electron impact and by decay of the upper excited states of xenon. A large part of the energy put into xenon excitation is therefore used in populating the resonant and metastable states. The resonant states quickly emit a UV photon at 147 nm while the metastable states undergo three body collisions to form excited molecular states of xenon (excimer). These molecular states emit UV photons in a continuum around 170 nm.

The global light efficiency of an AC PDP discharge cell is very low, on the order of 1 lm/W. This efficiency is a combination of the discharge efficiency in producing UV photons (on the order of 10%), the collection efficiency of the UV photons by the phosphors (about 40%), the efficiency of the UV-visible photons conversion (about 30%), the collection efficiency of the visible photons ($\approx 40\%$). This estimation gives an overall efficiency of 0.5%, roughly corresponding to 1 lm/W. An important part of the R&D on PDPs is therefore related to the improvement of the efficiency. There is obviously a need to improve the photon collection and the phosphor efficiency. It should also be possible to increase the discharge efficiency in producing UV photons. This is however, not an easy task because of other constraints. For example, it is easy to show that increasing the percentage of xenon in the mixture leads to a higher efficiency for UV production. However, an increase in xenon concentration leads to an increase in breakdown voltage (above 1% xenon), because of the low secondary electron emission coefficient of

xenon ions. A low operating voltage is necessary in PDPs in order to reduce the cost of the electronic drivers. The constraints which must be kept in mind when trying to optimize the efficiency of a PDP cell include: low operating voltage, non reactive gas mixture, low sputtering, simple electrode design and addressing, etc... The models have proved to be a very useful tool for understanding the influence of each parameter and to provide guidance toward optimization.

GLOW DISCHARGE MASS SPECTROMETRY

Glow discharge mass spectrometry (GDMS) is an analytical technique that is now widely used for elemental analysis of various materials [7–9]. This diagnostic uses a low current, glow discharge in a buffer gas (typically argon) to sputter atoms from a sample (usually the cathode or a substrate on the cathode) to be analyzed. Atoms of the sample are thus introduced into the gas phase. Some of these atoms are ionized in the discharge, and the ions are extracted through a small exit slit in the chamber wall leading to a mass spectrometer. The purpose of the calculations shown here was to investigate the effect of the cathode geometry on the ion current density distribution arriving at the plane of the exit slit leading to the mass spectrometer. The conditions we have chosen to study include those corresponding to the commercially available VG9000 spectrometer and Megacell source.

The physical and numerical model used for these calculations is the hybrid model briefly described above [10,11]. The fundamental variables are the electron and ion densities, and the potential (or electric field) distribution. These variables are functions of two dimensions in space (radial and axial directions, cylindrical symmetry is assumed) and of time. The charged particles are described with a fluid model in the drift-diffusion approximation, and Poisson's equations gives the distribution of the potential. The ionization source term is determined from a Monte Carlo simulation of the cathode-emitted electrons. The discharge voltage is input as a boundary condition, and discharge current is calculated from the solution for the densities and potential distribution

The 'pin' cathode discharge geometry used in these calculations is shown in Fig. 1. The cathode is cylindrical with a diameter of 0.3 cm and a length of 0.9 cm. The discharge chamber is 3.2 cm in diameter and 1.8 cm long. These dimensions and those used in the calculations with the 'disk' cathode geometry discussed below are summarized in Table 1.

We have calculated the steady-state charged particle density and self-consistent potential distributions at 0.3, 0.55 and 1.0 torr in argon in the pin geometry and at 0.55 torr for the disk cathode geometry. Table 1

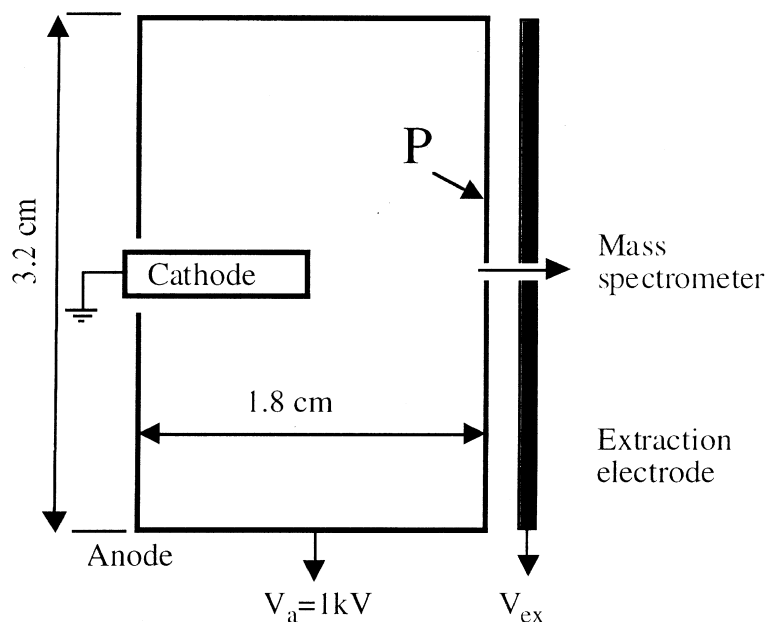


Fig. 1 Schematic of a glow discharge ion source for mass spectrometry.

Table 1 Summary of results from model calculations

Label	Pressure (torr)	Discharge geometry			V_d (Volts)	I_d (mA)	V_p (Volts)	n_p (cm^{-3})
		H(cm)	L(cm)	D(cm)				
A	0.3	1.8	0.9	0.3	999	0.09	1002	8.4×10^8
B	0.55	1.8	0.9	0.3	994	0.57	1002	1.95×10^{10}
C	1.0	1.8	0.9	0.3	968	3.18	975	4.67×10^{11}
D	0.55	1.8	0.3	0.9	992	0.82	1001	8.48×10^{10}
E	0.55	1.3	0.3	0.9	993	0.71	1001	3.25×10^{10}

The discharge geometry is defined by the cell height (H), the cathode length (L) and the cathode diameter (D). V_d and I_d are the discharge voltage and current, respectively, and V_p is the maximum potential in the discharge volume. The maximum ion density in the volume is n_p , and this is equal to the maximum electron density except at 0.3 torr (case A). Labels A, B and C correspond to the pin cathode geometry, and D and E correspond to the disk cathode geometry.

lists the anode voltage, V_d , the calculated discharge current, I_d , potential maximum in the discharge, V_p and the peak plasma, n_p , density for each of these cases.

Pin cathode geometry

Although the discharge conditions at 0.3 torr are not used for GDMS, the results at this pressure are included here to show the trends with increasing pressure (or current). At this low pressure, the calculated discharge current is 0.09 mA and space charge density only slightly distorts the geometrical potential distribution. The discharge current and plasma density increase to values more appropriate for GDMS as the pressure increases. At 0.55 torr the discharge current is 0.57 mA and the peak plasma density is $1.95 \times 10^{10} \text{ cm}^{-3}$. Increasing the pressure to 1 torr leads to a further increase in the discharge current (3.18 mA) and in the maximum plasma density ($4 \times 10^{11} \text{ cm}^{-3}$), and the quasi-neutral plasma region fills most of the volume. The high field sheath surrounding the cathode is consequently much thinner than for the lower pressures.

The ion current that can be drawn through the exit slit leading to the mass spectrometer depends on the ion current arriving at the plane of the exit slit (the vertical back surface of the chamber wall labeled P in Fig. 1). The calculated ion current density distributions along this surface P for 0.3, 0.55 and 1.0 torr argon are shown in Fig. 2 as a function of radial distance from the discharge axis. The ion current density reaching the plane P at 0.3 torr peaks off-axis. The current density distribution at the plane P is larger and much more uniform at 0.55 torr, but there is still an off-axis maximum. At 1.0 torr, the maximum ion current density in the plane P is on-axis. However, for this pin cathode geometry and for each of these pressures, the ion current density remains highest along the side wall and not at the plane of the exit slit.

Disk cathode geometry

The ion current arriving at the plane P of the exit slit can be enhanced by changing the geometry of the cathode. To show the effect of the cathode geometry on calculated discharge characteristics, we have changed the cathode dimensions to favor plasma formation in front of the cathode [12]. The cathode diameter was increased from 0.3 cm to 0.9 cm and its length decreased from 0.9 to 0.3 cm, thus increasing the cathode surface area by a factor of 3. We refer to this as the disk cathode geometry. To illustrate the effect of the cell geometry, we changed the spacing between the cathode face and the plane P by reducing the cell height from 1.8 cm to 1.3 cm and kept the larger diameter cathode. Both of these calculations were performed for argon at 0.55 torr.

The effect of changes in the geometry on the ion current density distribution at the plane P can be seen in Fig. 2. Changing from the pin to the disk cathode geometry causes an increase the magnitude of the ion current density arriving at the plane P on-axis by a factor of almost 10. A further slight increase is

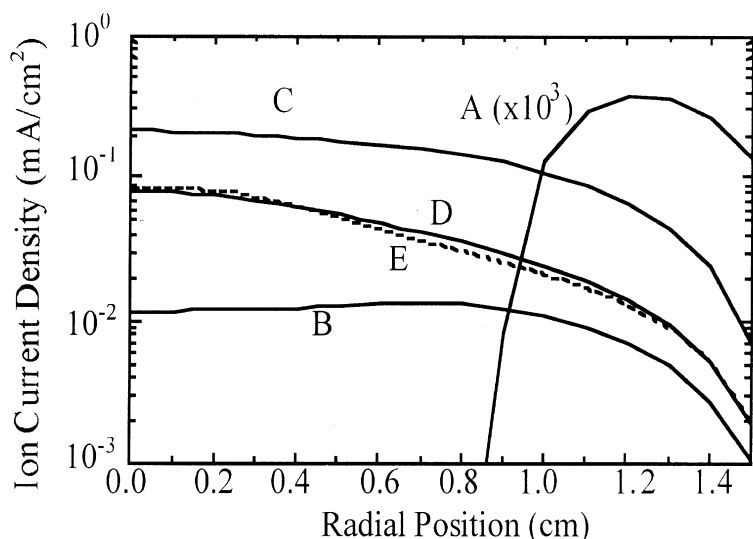


Fig. 2 Ion current density distribution along the back anode plane P as a function of distance from the axis. The labels of these curves correspond to the entries in Table 1; (A) pin geometry, 0.3 torr; (B) pin geometry, 0.55 torr; (C) pin geometry, 1.0 torr; (D) disk geometry, 0.55 torr; (E) disk geometry, 0.55 torr, reduced cell height (after [12]).

observed as the cell height is reduced from 1.8 to 1.3 cm. Thus, the sensitivity of this diagnostic technique can be improved by optimizing the cathode (sample) geometry.

The reasons for the increase in the ion current density at the plane P can be seen in Fig. 3 where contours of constant potential are shown at 0.55 torr for both cathode geometries. For the pin geometry, a quasi-neutral plasma region exists in a ring around the cathode, and a distinct high field sheath (closely spaced potential contours) appears around the cathode. The maximum potential in the discharge volume is several volts higher than the anode potential. The position of the potential maximum corresponds approximately at the position of the maximum plasma density. The disk geometry favors plasma

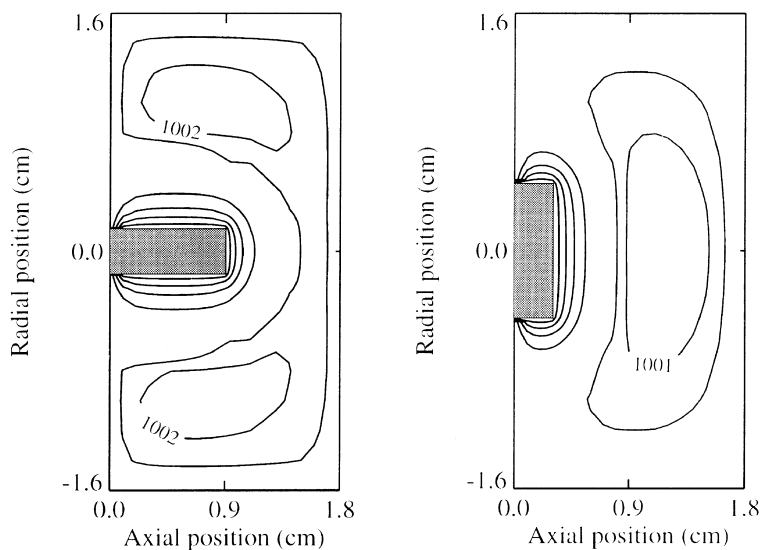


Fig. 3 Equipotential contours calculated for discharge in argon for two different cathode geometries (labels B and D in Table 1) for 0.55 torr argon. The contours are shown at intervals of 200 V between 0 and 1000 V, except for the contour labeled.

formation on-axis while the plasma forms a ring around the cathode in the pin geometry. Note that the total discharge currents for these two cases are not very different (from Table 1, 0.57 mA for the pin cathode geometry and 0.82 mA for the disk cathode geometry).

From Fig. 3, the electric field can be inferred; the field lines are normal to the equipotential contours. At the position of potential maximum, the electric field passes through zero and then changes sign on the other side of the maximum so as to inhibit electrons from leaving this region of positive space charge. Such a field inversion is typical in the negative glow of low-pressure discharges. It exists because of the nonlocal source of ionization. That is, electrons are emitted from the cathode (due to bombardment by ions) and are accelerated in the cathode fall. They deposit all or most of their energy in the form of ionization (and excitation) in the low field, negative glow at the end of the high field sheath. Similar to an externally sustained plasma, an ambipolar field exists in the negative glow plasma that goes through zero and changes sign. In the absence of a field reversal, the only ions that can reach the anode are those ions that are created in volume ionization events immediately in front of the anode. These few ions may reach the anode by diffusing against the field. Ions created closer to the cathode do not have enough energy to diffuse against the field to reach the anode. When there is a field reversal, the ions which can reach the anode are those which are created in ionization events on the anode side of the potential maximum. These ions are drawn by the field towards the anode. None of the ions created on the cathode side of the potential maximum can reach the anode. Note that the capability of a model to predict this field reversal depends on an accurate treatment of the nonlocal volume ionization.

The closed potential contours, indicating the presence of a field reversal, are centered on-axis in the disk cathode geometry. Ions produced near the axis on the anode side of the field reversal will be drawn toward the anode plane P and the radial electric field will tend to confine them near the axis, thus enhancing the ion current density reaching the plane P on-axis (the entrance to the mass spectrometer). Recall that none of the ions created in the plasma on the cathode side of the field reversal can reach the anode plane P. In the pin cathode geometry, the ionization source term (the number of electron-ion pairs created per unit volume and per unit time), as well as the maximum plasma density, form pronounced rings around the side of the cathode. The ionization source terms in the calculations with the larger cathode diameter peak on axis and on the cathode side of the field reversal, but they extend well into the anode side of the volume delimited by the zero field surface.

GAS TEMPERATURE

The results above for the GDMS were calculated supposing a constant neutral background gas temperature, or, equivalently, constant gas density because we fix the gas pressure. The neutral gas is heated by collisions (elastic and charge exchange) of the ions with the background gas. This is important in the cathode fall where the ion current is the dominant current component (gas heating due to elastic electron-neutral collisions is negligible). For typical glow discharge conditions, the ions deposit their energy in the gas (or in the cathode) far from the point in space where they gain the energy; the gas heating is nonlocal. To evaluate the assumption of a constant gas temperature, we have developed a Monte Carlo simulation of the heavy particle (ions and fast neutrals) and coupled this to our hybrid fluid model. The results of the hybrid model, the electric field profile, the ionization source term profile, and the current, are input to a particle model of the heavy particles.

From a series of parametric calculations in one-dimension which included also the effect of atoms sputtered from the cathode, we find that the gas heating in glow discharges due to the ion current in the sheath is far larger than that due to the thermalization of sputtered atoms from the cathode for discharge in argon with current density $< 20 \text{ mA/cm}^2$ at 1 torr [13]. The gas temperature is a maximum near the cathode, slightly outside the cathode fall. The shape of the temperature profile is more or less independent of the cathode temperature (assumed to be constant) and the accommodation coefficient (which quantifies the amount of energy absorbed by the cathode when particles are reflected from its surface), but these quantities determine the peak temperature.

Results from two-dimensional calculations of the gas temperature in the GDMS geometry are shown in Fig. 4 for the pin and disk cathode geometries at 0.55 torr argon. For a fixed voltage, the discharge current decreases when gas heating is taken into account. For the cases shown in Fig. 4, the current

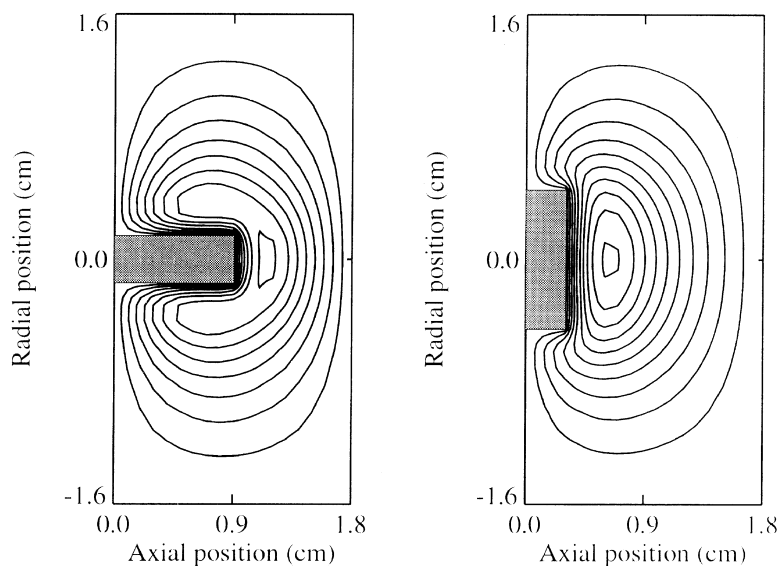


Fig. 4 Contours of constant gas temperature calculated for discharges in argon for two different cathode geometries (labels B and D in Table 1) for 0.55 torr argon. The contours are shown at intervals of 5 K between 305 and 340 K (for the pin geometry, B) and 350 K (for the disk geometry, D).

decreases about 20% when gas heating is included self-consistently in the calculations, but the potential and plasma density profiles change only slightly.

CONCLUSIONS

The two examples described in this paper show that modeling has become an extremely important tool for understanding and optimization of low temperature plasma devices. Simple models that do not include all the details involved in a practical device are also useful because they can provide a qualitative understanding of the device and guide optimization.

REFERENCES

- 1 J. P. Boeuf, C. Punset, A. Hirech H. Doyeux. *J. Phys IV France* **7**, C4–3 (1997); see also J. P. Boeuf, Th. Callegari, C. Punset, R. Ganter. *Workshop Digest of the 18th International Display Research Conference, Asia Display '98*, 209–220, SID (1998).
- 2 C. K. Birdsall. *IEEE Trans. Plasma Sci.* **19**, 65–85 (1991).
- 3 J. P. Boeuf, A. Merad. In *Plasma Processing of Semiconductors*, NATO ASI Series E. *Applied Sciences* (P. F. Williams, ed.), Vol. 336, pp. 291–320. Kluwer Academic (1997).
- 4 C. Punset, J. P. Boeuf, L. C. Pitchford. *J. Appl. Phys.* **83**, 1884–1897 (1998).
- 5 C. Punset, S. Cany, J. P. Boeuf. *J. Appl. Phys.* **86**, 124–133 (1999).
- 6 J. Meunier, P. Belenguer, J. P. Boeuf. *J. Appl. Phys.* **78**, 731–745 (1995).
- 7 J. A. C. Broekaert. In *Glow Discharge Spectroscopies* (R. K. Marcus, ed.). Plenum Press, New York (1993).
- 8 J. A. C. Broekaert. *Appl. Spec.* **49**, 12A–19A (1995).
- 9 W. W. Harrison. *J. Anal. At. Spect.* **3**, 867–872 (1988).
- 10 A. Fiala, L. C. Pitchford, J. P. Boeuf. *Phys. Rev. E* **49**, 5607–5622 (1994).
- 11 A. Fiala. Thesis de 3eme cycle. Université Paul Sabatier, Toulouse, France (1995).
- 12 A. Fiala, L. C. Pitchford, J. P. Boeuf, S. Baude. *Spectrochem. Acta* **B52**, 531–536 (1997).
- 13 I. Revel. Thesis de 3eme cycle. Université Paul Sabatier, Toulouse, France (1999).